

Structural and magnetic properties of lithium ferrite (LiFe_5O_8) thin films: Influence of substrate on the octahedral site order

Cihat Boyraz, Dipanjan Mazumdar, Milko Iliev, Vera Marinova, Jianxing Ma, Gopalan Srinivasan, and Arunava Gupta

Citation: *Applied Physics Letters* **98**, 012507 (2011); doi: 10.1063/1.3533908

View online: <http://dx.doi.org/10.1063/1.3533908>

View Table of Contents: <http://scitation.aip.org/content/aip/journal/apl/98/1?ver=pdfcov>

Published by the *AIP Publishing*

Articles you may be interested in

[Effect of silver addition on structural, electrical and magnetic properties of \$\text{Fe}_3\text{O}_4\$ thin films prepared by pulsed laser deposition](#)

J. Appl. Phys. **111**, 073907 (2012); 10.1063/1.3702463

[Large room temperature magnetization in nanocrystalline zinc ferrite thin films](#)

Appl. Phys. Lett. **88**, 262506 (2006); 10.1063/1.2217253

[Structural and magnetic properties of NiZn and Zn ferrite thin films obtained by laser ablation deposition](#)

J. Appl. Phys. **97**, 10G105 (2005); 10.1063/1.1854416

[Stress-induced magnetic anisotropy in thick oriented NiZn–ferrite films on \(100\) MgO substrates](#)

J. Appl. Phys. **81**, 6884 (1997); 10.1063/1.365249

[Static magnetic and microwave properties of Li-ferrite films prepared by pulsed laser deposition](#)

J. Appl. Phys. **81**, 4801 (1997); 10.1063/1.365468

High-Voltage Amplifiers

- Voltage Range from $\pm 50\text{V}$ to $\pm 60\text{kV}$
- Current to 25A

Electrostatic Voltmeters

- Contacting & Non-contacting
- Sensitive to 1mV
- Measure to 20kV



ENABLING RESEARCH AND INNOVATION IN DIELECTRICS, ELECTROSTATICS, MATERIALS, PLASMAS AND PIEZOS



www.trekinc.com

TREK, INC. 190 Walnut Street, Lockport, NY 14094 USA • Toll Free in USA 1-800-FOR-TREK • (t):716-438-7555 • (f):716-201-1804 • sales@trekinc.com

Structural and magnetic properties of lithium ferrite (LiFe_5O_8) thin films: Influence of substrate on the octahedral site order

Cihat Boyraz,^{1,2} Dipanjan Mazumdar,^{1,a)} Milko Iliev,³ Vera Marinova,⁴ Jianxing Ma,¹ Gopalan Srinivasan,⁵ and Arunava Gupta^{1,b)}

¹Center for Materials for Information Technology, University of Alabama, Tuscaloosa, Alabama 35487, USA

²Department of Physics, Faculty of Science and Letters, Marmara University, 34722 Istanbul, Turkey

³Department of Physics and Texas Center for Superconductivity, University of Houston, Houston, Texas 77204-5002, USA

⁴Institute for Optical Materials and Technologies, Bulgarian Academy of Sciences, 1113 Sofia, Bulgaria

⁵Department of Physics, Oakland University, Rochester, Michigan 49309-4401, USA

(Received 14 November 2010; accepted 6 December 2010; published online 4 January 2011)

Structural properties of lithium ferrite [LiFe_5O_8 , (LFO)] thin films are investigated as a function of substrate-induced strain and growth temperature. Through x-ray diffraction and Raman spectroscopy analysis we find LFO films grown on isostructural MgAl_2O_4 (MAO) are closer to bulk single crystal behavior, whereas the films remain coherently strained on lattice matched MgO substrate. Film texture and surface morphology are enhanced with better lattice match, indicating different growth modes on different substrates. Raman spectra reveal enhanced disorder of Li and Fe ions at the octahedral sites on MgO substrate contrasting with the relatively high degree of octahedral site ordering on MAO. © 2011 American Institute of Physics. [doi:10.1063/1.3533908]

Lithium and related substituted ferrites [LiFe_5O_8 , (LFO)] have attracted continual interest because of their technological applications as potential cathode materials in lithium-ion batteries and as components of microwave devices such as gyrators, phase shifters, circulars, and isolators.^{1–3} With a high Curie temperature of 950 K and high saturation magnetization (2.5 $\mu\text{B}/\text{formula unit}$), ultrathin films of LFO could have potential use in the emerging area of spintronics where the demand for magnetic insulators has enjoyed renewed interest for applications related to the spin-filtering effect.^{4–6} In the bulk form, LFO structure conforms to the inverse spinel structure, where the tetrahedral sites are filled by Fe^{3+} , and Li^+ and Fe^{3+} share the octahedral sites. Structurally, LFO exists in two crystallographic phases, namely, the ordered α (space group $P4_132$) and disordered β phase (space group $Fd3m$).⁷ In the ordered phase, the Li^+ and Fe^{3+} ions occupy the octahedral sites in 1:3 ratio, whereas in the disordered phase these ions are distributed randomly. The α -LFO has a primitive cubic unit cell with $a=c=8.33 \text{ \AA}$ and undergoes an order-disorder transition close to 750 °C.⁸ One of the consistent problems confronted in replicating bulklike properties for spinels into thin films can partly be attributed to the lack of isostructural substrates with good lattice match. The preferred substrate for LFO has been rock salt MgO for better lattice match.^{9,10} However, from our recent experience, the use of MgAl_2O_4 (MAO), a spinel substrate, coupled with low pressure growth has reproduced bulklike properties for other isostructural ferrite materials such as NiFe_2O_4 and CoFe_2O_4 .¹¹

In this study, we have fabricated LFO films using the pulsed laser deposition technique (excimer laser, $\lambda=248 \text{ nm}$) on (100)-oriented cubic substrates [MAO , MgO , and SrTiO_3 (STO)] with different structure and lattice constants. Compared to bulk LFO, rocksalt MgO substrate offers

a tensile strain of +1.1%, whereas spinel MAO and perovskite STO offer a compressive strain of -3.0% and -6.2% , respectively. Coupled with the substrate study, we have grown LFO at different temperatures to suitably investigate the optimum growth conditions and growth mode. All LFO films were grown at a fixed 10 mTorr background oxygen pressure, under identical laser energy conditions of approximately 1.5 J/cm^2 with a repetition rate of 10 Hz. Prior to deposition, the substrates were heated to 700 °C and maintained at that temperature for 4 h. After growth, the samples were cooled slowly at a rate of 10–15 °C/min at 100 mTorr to room temperature. Surface morphology was investigated using a Veeco nanoscope atomic force microscope (AFM). To determine the phase and epitaxy of the films, a standard θ -2 θ x-ray diffraction setup (Phillips X'pert Pro) was used with a Cu $K\alpha$ source operating at 45 kV and 40 mA. Magnetic properties of the LFO films were determined by a superconducting quantum interference device (SQUID) magnetometer and alternating gradient magnetometer. Polarized Raman spectra were measured with XX, XY, X'X', and X'Y' scattering configurations using 488 nm excitation. In these notations the first and second letters refer to the polarization direction of the incident and scattered light, respectively. X, Y, X', and Y' corresponding to the [100], [010], [110], and $[-110]$ cubic directions.

Detailed texture and epitaxy analysis included symmetric θ -2 θ scans, rocking curves, and x-ray-reflectivity. All films in the study had thickness of between 120 and 160 nm. Large-angle θ -2 θ scans show only diffraction peaks corresponding to LFO films and the substrates. No evidence of any secondary phase is found from x-ray measurements. Figures 1(a)–1(c) show θ -2 θ plots around the (004) peak for LFO films on MgO , MAO, and STO grown at different temperatures. From the film reflection intensity and rocking curve analysis we conclude that the samples grown at 610 °C to have the best texture on all substrates. Films on MAO and STO show nearly bulk lattice parameters [Fig.

^{a)}Electronic mail: dmazumdar@mint.ua.edu.

^{b)}Electronic mail: agupta@mint.ua.edu.

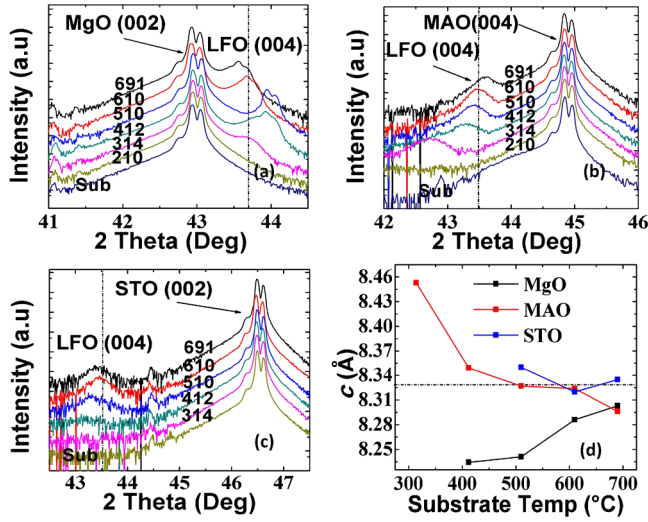


FIG. 1. (Color online) X-ray diffraction θ - 2θ scans of LFO films grown at different temperatures on (a) MgO, (b) MAO, and (c) STO substrates. (d) Growth temperature dependences of the determined lattice constants in the film normal direction. Dashed lines in all figures correspond to bulk LFO lattice constant (8.33 Å).

1(d)], which indicates strain relaxation. At higher temperatures, both the intensity and texture deteriorate on all substrates, probably from defects in the films likely from Li loss. The trend in the out-of-plane lattice parameter, as shown in Fig. 1(d), is consistent with the strain relationship with the substrate. Surprisingly, even though the sample on MgO shows the best texture (full-width-at-half-maxima of 0.04°) compared to MAO ($\sim 0.60^\circ$) or STO ($\sim 1.60^\circ$) it is still far from the bulk values. To analyze further, we measured the in-plane lattice parameter of only the LFO film on MgO substrate using Cohen's method as shown in Table I.^{12,13} We find that even at the highest temperature (690 °C), the MgO films are significantly strained to the substrate ($2a_{\text{MgO}} = 8.42$ Å). A slight increase in the cell volume with temperature is observed and a positive Poisson ratio value is obtained in all our films as expected.

Surface morphology of LFO films show that samples grown on STO substrate [Fig. 2(c)] have higher rms roughness than MAO [Fig. 2(b)] or MgO [Fig. 2(a)] substrate. The samples grown on MgO are practically atomically flat at all growth temperatures. Further, the roughness on STO substrates increases with temperature, whereas samples on MgO and MAO did not show this trend consistently. We speculate that the LFO films grow in a two-dimensional layer-by-layer mode on MgO and MAO substrate, whereas the films on STO grow predominantly in three-dimensional island mode. Lattice mismatch is playing a significant role here in the growth mode, as has been reported in other systems.¹⁴

TABLE I. Unit-cell lattice parameters and Poisson ratio values of strained LFO films grown on MgO substrate at different temperatures.

Growth temperature (°C)	In-plane lattice parameter (a) (Å)	Out of plane lattice parameter (c) (Å)	Volume $a^2 \times c$ (Å ³)	Poisson's ratio $-\left(\frac{c - \text{bulk}}{a - \text{bulk}}\right)$
690	8.434	8.303	590.61	0.26
610	8.428	8.290	588.85	0.41
510	8.414	8.244	583.64	1.02
412	8.414	8.236	583.07	1.12

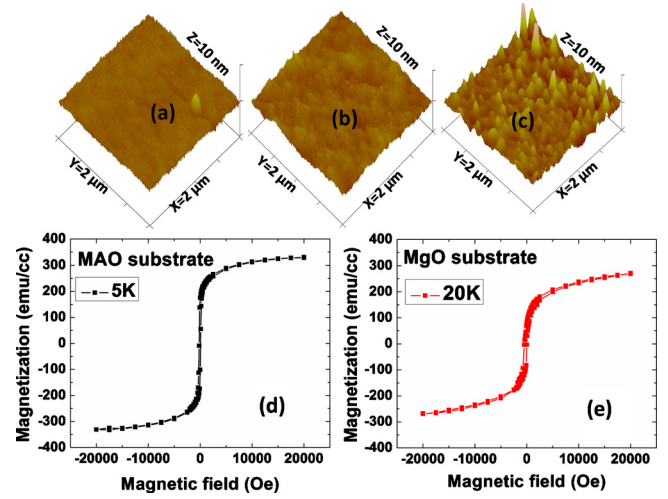


FIG. 2. (Color online) $2 \mu\text{m} \times 2 \mu\text{m}$ AFM images of LFO films grown at 610°C on (a) MgO, (b) MAO, and (c) STO substrates. The vertical scale is 10 nm in all figures. The rms roughness values are 0.18, 0.26, and 2.9 nm on MgO, MAO, and STO substrates, respectively. (d) and (e) SQUID measurement of the LFO film on (d) MAO and (e) MgO substrate. Films on MAO substrate show near bulk magnetization values.

Magnetic measurements are shown in Figs. 2(d) and 2(e) for samples grown at 610°C on MAO and MgO. The data on MgO sample were taken at 20 K where the magnetic contribution of the substrate was measured to be negligible. After proper substrate correction, we found that the sample on MAO has close to bulk magnetization value ($2.5 \mu\text{B}/\text{formula unit} \sim 320 \text{ emu/cc}$). The sample on MgO substrate had much lower magnetization and did not appear to saturate at high fields. This could imply the formation of strong antiphase boundaries which have been reported in other spinel films.¹⁵⁻¹⁷

In Fig. 3 are compared the polarized Raman spectra of LFO single crystal and LFO/MAO and LFO/MgO films. From symmetry considerations one expects large number of Raman allowed phonon modes, $6A_1 + 14E + 20F_2$, in the ordered α -phase ($P4_132$), compared to only five ($A_{1g} + E_g + 3F_2$) in the disordered β -phase ($Fd3m$). The $A_1(A_{1g})$ modes are allowed in the XX and X'X' spectra, the $E(E_g)$ modes—in XX and X'Y', and $F_2(F_{2g})$ modes—in the X'X' and XY spectra, and therefore the symmetry of Raman lines can unambiguously be identified from their polarization dependence. The comparison clearly shows that the spectra of LFO/MAO films reproduce to a great extent that of the ordered single crystal, although the lines are definitely broader. On the other hand, the spectra of LFO/MgO exhibit only the Raman lines expected for the $Fd3m$ phase, which indicates complete disorder of Li and Fe at the octahedral (B)-sites. This result is of significant interest as it shows that the non-

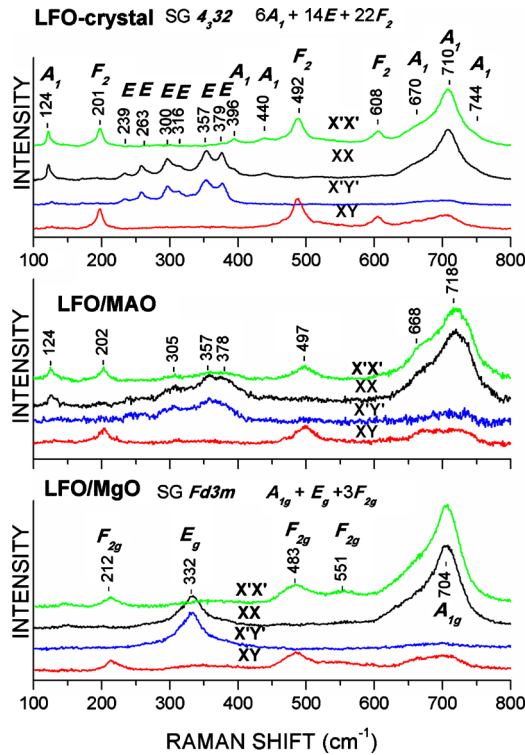


FIG. 3. (Color online) Polarized Raman spectra of LFO single crystal and LFO/MAO and LFO/MgO films as obtained with 488 nm laser excitation at room temperature.

equilibrium laser ablation process used for film growth mimics the rapid quenching method⁷ used to stabilize the β -phase in the bulk. Thus the pulsed laser deposition technique provides a convenient route for the preparation of unique samples of β -phase LFO films. It is worth mentioning here that the x-ray diffraction and Raman spectroscopy are sensitive to different ordering scales, long and short range orders, respectively. Therefore, a conclusion can be made that the LFO/MgO films reported here are examples of true β -phase LFO. Raman spectra of LFO/STO indicate the presence of α -Fe₂O₃, not picked up by x-ray diffraction, along with ordered alpha-phase LFO.

In summary, we have investigated LFO thin films under different substrate-induced strain and provide strong evi-

dence for partial ordering of Li and Fe at the octahedral sites of LFO/MAO and complete octahedral-site disorder of the LFO/MgO films. Even though texture, epitaxy, and growth mode improved with lattice matching, structural and magnetic properties are significantly closer to single crystal for the case of isostructural MAO. Our study provides unique opportunity for further studies of the disordered β -phase of LiFe₅O₈ in the thin film form at room temperature for energy applications.

This work was supported by ONR Grant No. N00014-09-0119, by the State of Texas through the Texas Center for Superconductivity at the University of Houston, and partly by Contract Nos. DO 02-167/2008 and TK-X-1712/2007 of the Bulgarian National Scientific Research Fund.

- ¹H. M. Widatallah, C. Johnson, F. Berry, and M. Pekala, *Solid State Commun.* **120**, 171 (2001).
- ²G. M. Argentina and P. D. Baba, *IEEE Trans. Microwave Theory Tech.* **22**, 652 (1974).
- ³J. S. Baijal, S. Phanjoubam, D. Kothari, C. Prakash, and P. Kishan, *Solid State Commun.* **83**, 679 (1992).
- ⁴U. Lüders, A. Barthélémy, M. Bibes, K. Bouzehouane, S. Fusil, E. Jacquet, J.-P. Contour, J.-F. Bobo, J. Fontcuberta, and A. Fert, *Adv. Mater.* **18**, 1733 (2006).
- ⁵M. G. Chapline and S. X. Wang, *Phys. Rev. B* **74**, 014418 (2006).
- ⁶A. V. Ramos, M.-J. Guittet, J.-B. Moussy, R. Mattana, C. Deranlot, F. Petroff, and C. Gatel, *Appl. Phys. Lett.* **91**, 122107 (2007).
- ⁷P. Braun, *Nature (London)* **170**, 1123 (1952).
- ⁸J. L. Dormann, A. Tomas, and M. Nogues, *Phys. Status Solidi A* **77**, 611 (1983).
- ⁹G. Balestrino, S. Martellucci, A. Paoletti, P. Paroli, G. Petrocelli, A. Tebano, S. A. Oliver, and C. Vittoria, *Solid State Commun.* **96**, 997 (1995).
- ¹⁰Y.-Y. Song, M. S. Grinolds, P. Krivosik, and C. E. Patton, *J. Appl. Phys.* **97**, 103516 (2005).
- ¹¹J. X. Ma, D. Mazumdar, G. Kim, H. Sato, N. Z. Bao, and A. Gupta, *J. Appl. Phys.* **108**, 063917 (2010).
- ¹²M. U. Cohen, *Rev. Sci. Instrum.* **6**, 68 (1935).
- ¹³S. Okamoto, O. Kitakami, and Y. Shimada, *J. Magn. Magn. Mater.* **208**, 102 (2000).
- ¹⁴F. K. LeGoues, M. Copel, and R. Tromp, *Phys. Rev. Lett.* **63**, 1826 (1989).
- ¹⁵M. Luysberg, R. G. S. Sofin, S. K. Arora, and I. V. Shvets, *Phys. Rev. B* **80**, 024111 (2009).
- ¹⁶D. T. Margulies, F. T. Parker, M. L. Rudee, F. E. Spada, J. N. Chapman, P. R. Aitchison, and A. E. Berkowitz, *Phys. Rev. Lett.* **79**, 5162 (1997).
- ¹⁷R. Datta, S. Kanuri, S. V. Karthik, D. Mazumdar, J. X. Ma, and A. Gupta, *Appl. Phys. Lett.* **97**, 071907 (2010).